We are IntechOpen, the world's leading publisher of Open Access books Built by scientists, for scientists

Chapter

Production of the ^{103}Pd via Cyclotron and Preparation of the Brachytherapy Seed

Pooneh Saidi and Mahdi Sadeghi

Abstract

This study will briefly explain the production of ^{103}Pd via cyclotron for brachytherapy use. The excitation functions of ^{103}Rh(p,n)^{103}Pd and ^{103}Rh(d,2n)^{103}Pd reactions were calculated using ALICE/91, ALICE/ASH, and TALYS-1.2 codes and compared with published data. Production of ^{103}Pd was done via ^{103}Rh(p,n)^{103}Pd nuclear reaction. The target was bombarded with 18 MeV protons at 200 μA beam current for 15 h. After irradiation and radiochemical separation of the electroplated rhodium target, at the optimum condition, ^{103}Pd was absorbed into Amberlite®IR-93 resin. The preparation of the brachytherapy seed, which is loaded by the resin beads, has also been presented. At least, the method to determine the dosimetric parameters for the seed by experimental measurement has been presented.

Keywords: brachytherapy, cyclotron, production, cross-section, excitation function, palladium, rhodium

1. Introduction

Cyclotrons are charged particle circular accelerators. They are a type of particle accelerator that has many applications in nuclear physics, industry, technology, and medicine. They play an important role in medicine; for example, they are used for radiation therapy, production of medical radioisotopes, and biomedical research [1]. As a particle accelerator, one of the important uses of the cyclotron in medicine is radioisotope production [2].

For a long period, radioisotope production is basically done in nuclear reactors, but their availability is slowly decreasing, and due to some advantages of radioisotope production with the cyclotron, the development of particle accelerators started in the past century, so accelerator-based production facilities are growing, and various radioisotopes suitable for medical applications are produced.

In this chapter, the production method for the radioisotope, Palladium-103 (^{103}Pd), via cyclotron is discussed. Palladium-103 with energy emission about 20 keV results in the rapid dose falloff with the distance which is suitable for low-dose-rate (LDR) brachytherapy [3]. For nearly 25 years, brachytherapy sources containing ^{103}Pd have been clinically introduced and are in use [4, 5]. Sources containing ^{103}Pd are most commonly used in the treatment of prostate and eye cancer [6–8].

Radionuclide	$T_{1/2}$	Mode of decay	The energy of the emitted particle (keV)
^{32}P	14.26 d	β^-(100)	690
^{137}Cs	30.04 y	β^-(100)	662
^{198}Ir	73.8	β^-(95.34)	380
^{198}Au	2.69	β^-(100)	412
^{125}I	59.4 d	EC (100)	28
^{169}Yb	32.02 d	EC (100)	93
^{103}Pd	16.99 d	EC (100)	21
^{153}Sm	46.28 h	β^-(100)	223
^{142}Pr	19.12	β^-(96.3)	809
^{170}Tm	128.6 d	β^-(99.87)	66.39

Table 1.
Examples of radioisotopes commonly used in brachytherapy.

Brachytherapy is a form of treatment where a sealed radioactive source placed on or in the tissue/tumor is to be irradiated. With this method, a high dose can be delivered to the tumor with a rapid decrease in dose in the surrounding normal tissue. Brachytherapy sources are usually encapsulated; the encapsulated sources are placed within the body cavities close to the tumor, in a lumen of organs, or implanted into the tumor or placed over the tissue to be radiated.

Depending on the source dose rate, brachytherapy sources are classified into three categories [9]:

- High-dose-rate sources (HDR): >12 Gy/h radioisotopes with high-energy photon emitters like ^{137}Cs, ^{60}Co, ^{192}Ir, and ^{198}Au are used.

- Medium-dose-rate sources (MDR): 2–12 Gy/h radioisotopes are used; this category is not commonly used in brachytherapy.

- Low-dose-rate sources (LDR): Less than 2 Gy/h radioisotopes with low-energy photon emitters like ^{103}Pd and ^{125}I are used.

Table 1 shows examples of radioisotopes commonly used in brachytherapy for the three mentioned categories [10].

This study will briefly explain the production of the ^{103}Pd via cyclotron and will shortly describe some detail of ^{103}Pd production such as production process, targetry, radiochemical separation, seed fabrication, and seed dosimetry method.

2. Materials and methods

2.1 Cyclotron production of ^{103}Pd

There are different methods for the production of ^{103}Pd via cyclotron. Two of them are $^{103}Rh(p,n)^{103}Pd$ and $^{103}Rh(d,2n)^{103}Pd$ [3]. In this study, the excitation functions for both reactions have been calculated, and the optimum condition for each reaction has been obtained. Experimental data for the proton bombardment on rhodium metal as the target, via $^{103}Rh(p,n)^{103}Pd$ reaction, has also been measured. Rhodium target has been bombarded by proton in a cyclotron (Cyclone-30, IBA) with 18 MeV energy and a beam current intensity of 200 μA at the Agricultural, Medical and Industrial Research School (AMIRS) [11].

To achieve the ^{103}Pd from the irradiated target, the radiochemical separation stage is started. The problem in this stage is the dissolution of target material due to the extremely low chemical reactivity of rhodium metal. The other problem is the high quantity of rhodium in the solution. A well-known palladium extractor is dimethylglyoxime, but to prevent the decrease of extraction yield, α-furyldioxime has been used [12]. Purely obtained ^{103}Pd is then absorbed into resin; the active resins are encapsulated inside the titanium casing.

2.2 Calculation of excitation function

Excitation functions of the ^{103}Rh(p,n)^{103}Pd and ^{103}Rh(d,2n)^{103}Pd reactions were calculated using ALICE/ASH, EMPIRE (version 3.1 Rivoli) and TALYS-1.2 nuclear codes, and the TENDL-2010. Using the codes simultaneously increases the accuracy of calculations. The calculated results were compared to the existing data of references [13–18].

2.3 Nuclear models applied for cross-section calculations

The ALICE/ASH code: This code is a modified version of the ALICE code, and to describe the pre-equilibrium particle emission from nuclei, the geometry-dependent hybrid model (GDH) is used. Calculations were carried out based on the Fermi gas model with the nuclear level density parameter $a = A/y$ and the generalized superfluid nuclear model. The default value of y is equal to [17, 19].

The TALYS code: TALYS is a computer code developed at NRG Petten and CEA to predict and analyze the nuclear reactions. TALYS models the nuclear reactions that involve protons, deuterons, neutrons, alpha particles, gamma rays, tritons, and hellions. The code simulated the reactions in the energy range from 1 keV to 200 MeV, for target nuclides of mass 12 and heavier [14, 17].

EMPIRE: EMPIRE (version 3.1 Rivoli) simulates various nuclear reactions, over a broad range of energies and incident particles. This system can be used for nuclear data evaluation and also for the theoretical calculation of nuclear reactions. A projectile can be a photon, a nucleon, and light or heavy ion. There is a broad range of energy in the system; the energy range starts just above the resonance region in the case of a neutron projectile and extends up to a few hundred MeV for heavy ion-induced reactions [20].

2.4 The thickness of the target

The required thickness of the target has been calculated via the stopping and range of ions in matter (SRIM) code [21]. Based on the code results, to take full advantage of the excitation function and also to avoid the production of the radioisotope impurity, the entrance energy of the proton should be 18 MeV. The physical thickness of the rhodium layer is chosen in such a way that for a given beam/target angle geometry, the particle exit energy should be 6 MeV. The thickness of the rhodium target has to be 475 μm for 90° geometry. To minimize the thickness of the rhodium layer (and hence lower the cost price per target), a 6° geometry is preferred; in this case, the thickness of the target decreases, and a 45–50 μm layer is sufficient.

Identification of the gamma ray emitting from the radionuclides is performed by using gamma-ray spectroscopy with a high-purity germanium HP(Ge) detector (Canberra™ model GC1020-7500SL).

2.5 Preparation of ^{103}Pd brachytherapy seeds

After irradiation, the radiochemical separation phase has been started. In this phase, the $PdCl_2$ solution has been separated from rhodium, zinc, and copper.

According to the brachytherapy seed model (in case of using a sphere made of resin), resin beads and marker are encapsulated inside the titanium capsule. The end caps of the capsule are welded precisely to prevent source leakage [22]. Regarding the physical design and configuration of the source internal component, two types of designs have been used: (a) rod/wire/cylinder made of ceramic, glass, or high-Z materials and (b) sphere made of resin. In this study sphere design of the source has been discussed.

Figure 1 shows a schematic diagram of eight different brachytherapy seeds which are designed at the Agricultural, Medical, and Industrial Research School [7, 23–25].

2.6 Dosimetry of the seed

According to the American Association of Physicists in Medicine (AAPM) Radiation Therapy Committee recommendation, the dosimetry characteristics

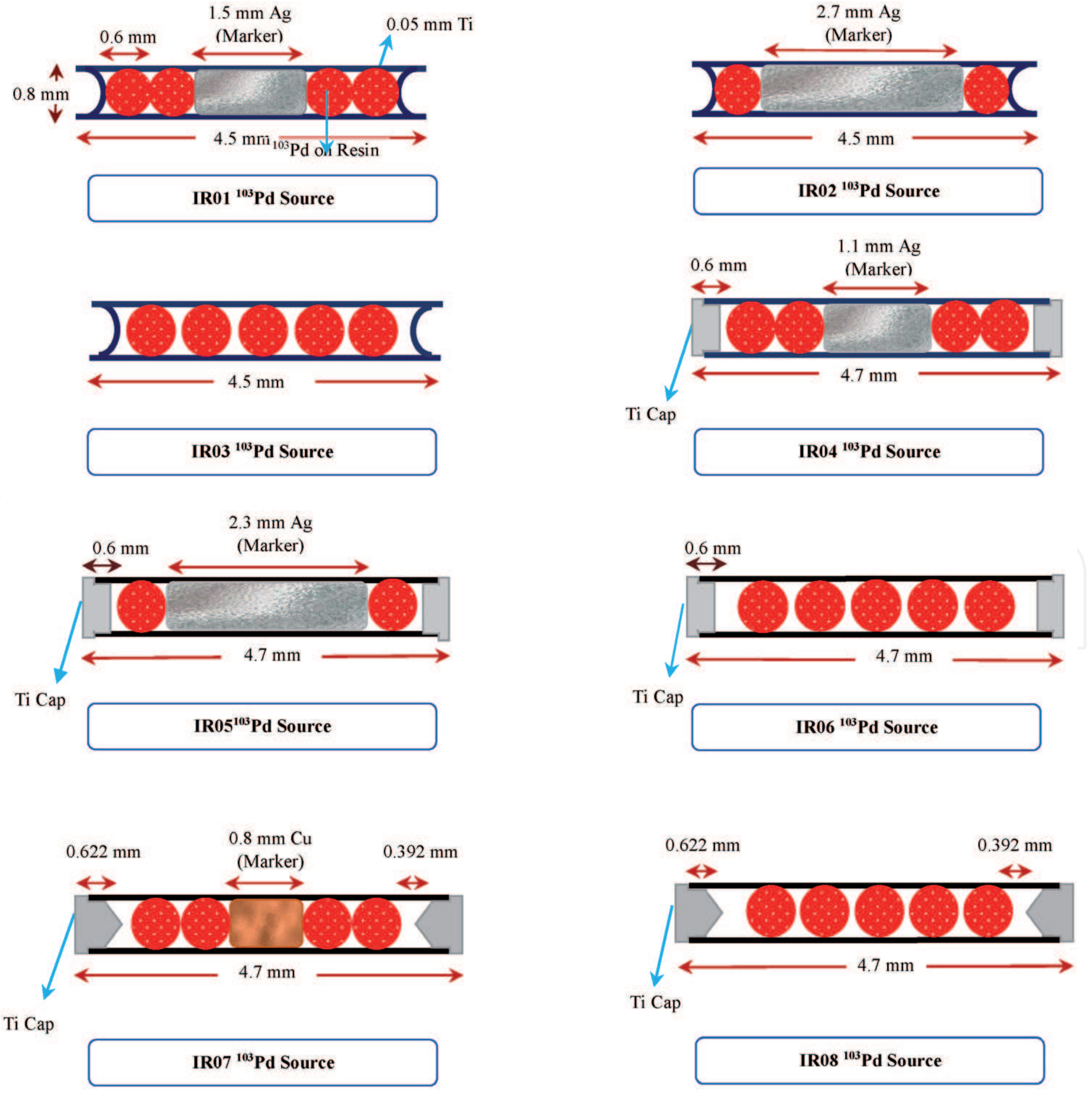

Figure 1.
Schematic drawing of the designed ^{103}Pd sources.

for all new interstitial brachytherapy seeds with energies less than 50 keV should be investigated by two independent investigators, theoretical calculations and experimental measurements. This work presents the method for thermoluminescent dosimeter (TLD) measurements to determine the dosimetric characteristics of the brachytherapy seed containing resin beads. The TLD-GR200A thermoluminescent dosimeters and two Perspex phantoms have been used, one Perspex phantom for the anisotropy function, $F(r, \theta)$, and the other for the radial dose function, $g_L(r)$.

3. Results and discussion

3.1 Excitation function

3.1.1 Excitation function study of ^{103}Rh(p,n)^{103}Pd reaction

The evaluation of the acquired data from the codes showed that the best range of the energy for proton in the ^{103}Rh(p,n)^{103}Pd reaction is 18–8 MeV. The maximum cross-section by EMPIRE (version 3.1 Rivoli) code is at E_p = 10 MeV, and the value is 574.44 mb. To evaluate the obtained results, **Figure 2** shows the comparison between the calculated results in this study and measured data by others. For the ^{103}Rh(p,n)^{103}Pd reaction, there are five cross-section measurements that exist in the literature by authors of references [26–29].

The calculated results from the TENDL-201, TALYS-1.2, and ALICE/ASH codes are in acceptable agreement with the measured data from [29], and calculated results from EMPIRE (version 3.1 Rivoli) code are in good agreement with the Hermanne et al. measured data (**Figure 2**).

3.1.2 Excitation function study of ^{103}Rh(d,2n)^{103}Pd reaction

According to the results from the codes, the optimum range of energy of the deuteron particle to produce ^{103}Pd from ^{103}Rh target for the ^{103}Rh(d,2n)^{103}Pd reaction is 22 to 8 MeV. The obtained results from ALICE/ASH hybrid model

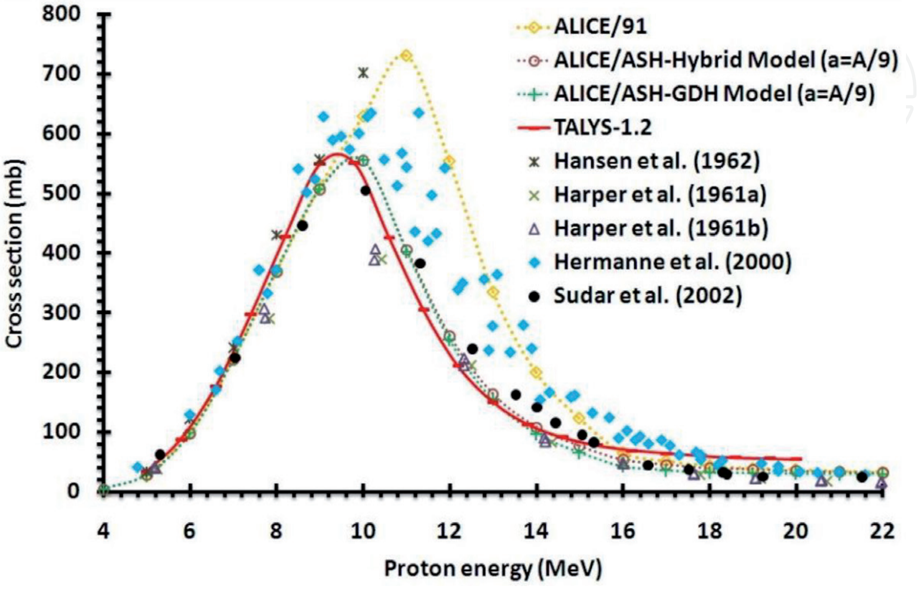

Figure 2.
Excitation function of ^{103}Rh(p,n)^{103}Pd reaction by ALICE/91, ALICE/ASH and TALYS-1.2 codes, and experimental data [10].

(a = A/9) show that the maximum cross-section is 1158.795 mb (Ed = 13 MeV). Comparison between the calculated results of this study and the measured data obtained by [30, 31] is presented in **Figure 3**.

The obtained results from ALICE/ASH code are in good agreement with the measured data by Hermanne et al. up to 20 MeV, whereas TALYS-1.2 and EMPIRE (version 3.1 Rivoli) calculated results have lower values than ALICE/ASH results and also experimental data.

3.2 Production of ^{103}Pd

To prepare the rhodium target for irradiation, via the electrodeposition process, a thick layer of rhodium has been placed of the copper backing. According to Sadeghi et al. study [11, 12], the following conditions are the optimum conditions for the electrodeposition:

- 4.8 g rhodium (as $Rh_2(SO_4)_3$)
- pH = 2
- DC current density of 8.5 mA cm^{-2}
- 1% sulfamic acid (w/v)
- Temperature 40–60°C

After the electrodeposition process, the adhesion quality of the rhodium layer on the target backing has been tested by the thermal shock. The thermal shock has been carried out by heating the target up to 500°C for 1 h (The temperature that the Rh layer experience during high current irradiation). Thereafter, the hot target is submerged in cold water in a temperature of about 15°C. Observation of neither crack formation nor peeling off of the rhodium layers indicated a good adhesion for the purpose.

Afterward, the rhodium target was bombarded with 18 MeV protons at 200 μA beam current for 15 h (3000 μAh) [12]. At the end of the bombardment (EOB),

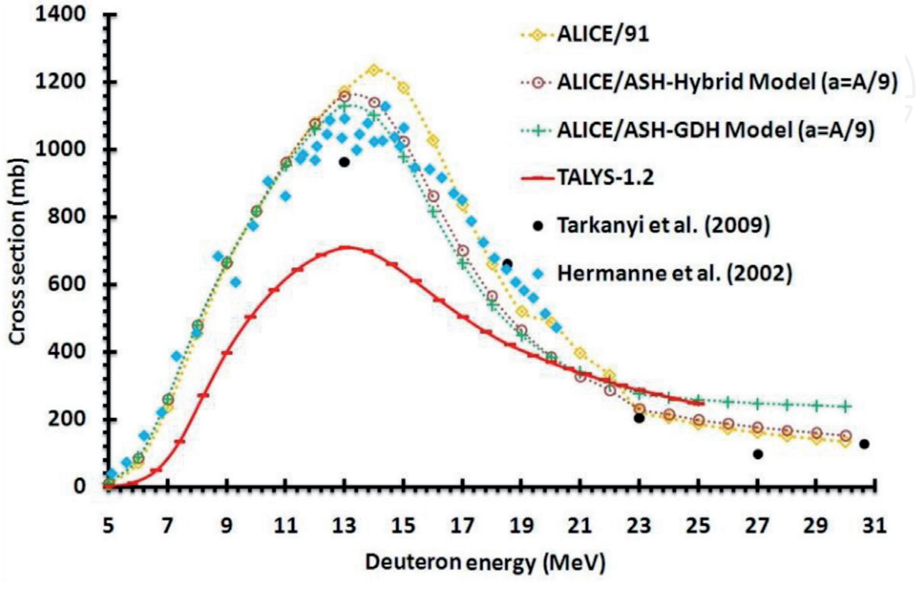

Figure 3.
Excitation function of ^{103}Rh(d,2n)^{103}Pd reaction by ALICE/91, ALICE/ASH and TALYS-1.2 codes, and experimental data [10].

the activity of ^{103}Pd and the yield of production are 685 mCi and 8.44 MBq/lAh, respectively. After the proton bombardment, the dissolution process has been started.

The optimum conditions of the electro-dissolution are as follows:

- 12 N HCl solution
- AC current density > 1.8 A cm^2
- Temperature: 75°C

After the dissolution of the target from copper backing, the residual contains $PdCl_2$, rhodium, zinc, and copper, so during the radiochemical separation phase, the $PdCl_2$ solution should be separated from rhodium, zinc, and copper. According to the data in **Figure 4**, the purity of the obtained radio-palladium is about 99%. Thereafter, the obtained filtrate solution was loaded onto the column of size Ø 0.5 cm × 2 cm packed with Amberlite®IR-93 resin with 0.6 mm diameter. The summarized results in **Figure 5** show that 0.05 M HCl is the most suitable concentration for adsorption of ^{103}Pd on the Amberlite®IR-93 resin.

The dosimetric parameters of the seeds have been determined by theoretical calculation and experimental measurement, according to TG-43 U1 report. The theoretical method to obtain the dosimetric parameters of the brachytherapy seeds has been discussed and explained in Refs.s [6, 9].

The following is the method to determine the dosimetric parameters by experimental measurements.

3.3 Dosimetry method

3.3.1 Thermoluminescent dosimeters

The TLD-GR200A (PTW, Freiburg, Germany) circular chips [26] of the following specifications have been used in this study:

- 0.8 mm thickness
- 4.5 mm in diameter

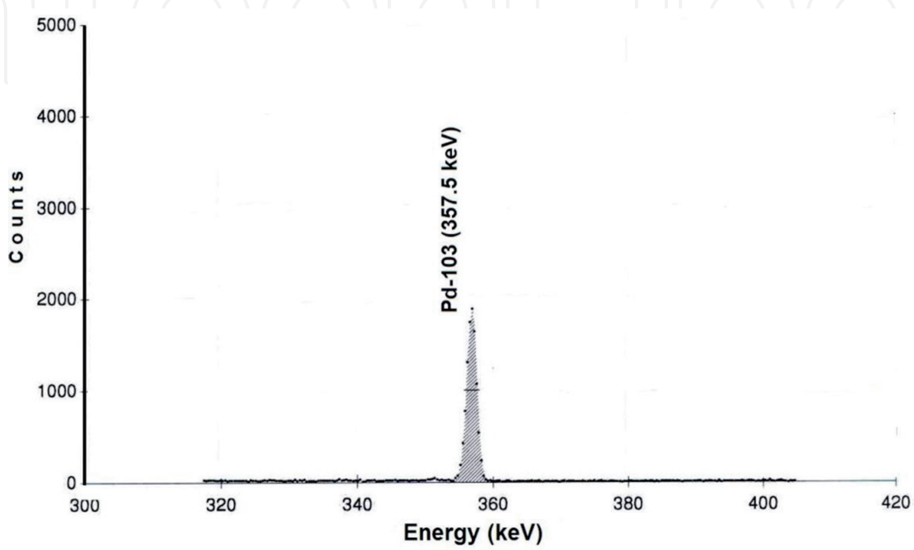

Figure 4.
HPGe spectrum of radiochemically separated ^{103}*Pd [10].*

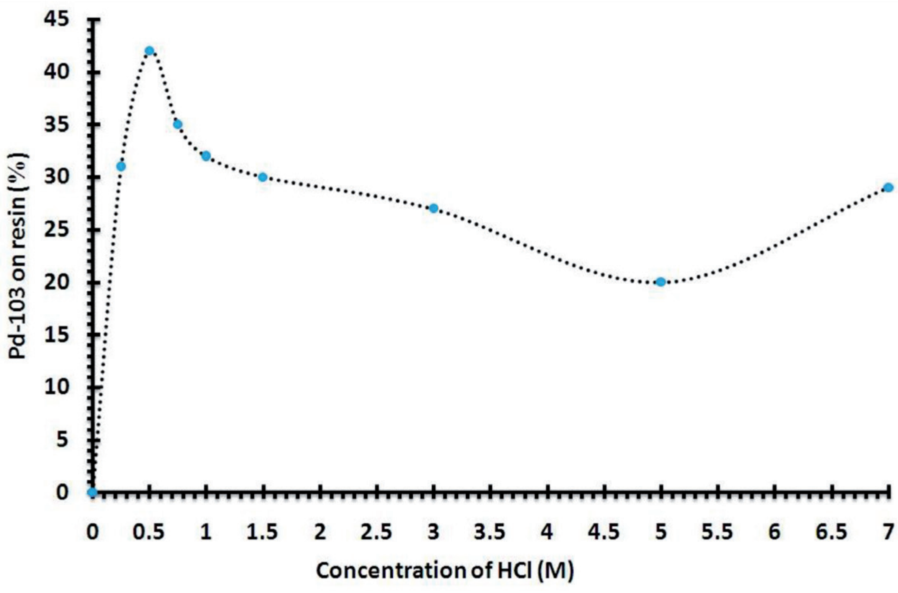

Figure 5.
Absorption profile of ^{103}Pd, as a function of HCl concentration on Amberlite®IR-93 resin [10].

For the TLD calibration, before each experimental measurement, the entire batch of TLDs is exposed to a calibrated Cobalt-60 standard beam. The variation of response of the TLDs to the same exposure is tracked by normalizing the individual TLD readings to the average value.

The irradiated TLDs (irradiated by the brachytherapy seed in the phantom) are read using a KFKI RMKI TLD reader (KFKI Research Institute of the Hungarian Academy of Sciences, Budapest, Hungary), and then they are annealed by heating at 240°C for 10 min followed by fast cooling. The responses of the TLD have to be corrected for background. This is done by subtracting the average response of background TLDs from the responses of all other TLDs in each measurement [25, 32].

3.3.2 Phantoms

To determine the dosimetric parameters of the seeds by experimental measurement, the phantom of Perspex slabs (**Figure 6**), by the following specification, has been used.

- Dimension: 30 cm × 30 cm × 15 cm
- Composition (by weight percent): H, 8%; C, 60%; and O, 32%
- Density: 1.19 g/cm^3

The design of the two phantoms to measure the radial dose and anisotropy functions are based on those of [25].

Figure 7 shows the phantom slab which is used for the experimental measurements of the brachytherapy seed radial dose function values. As shown in **Figure 7**, in the central phantom slaps, the holes are drilled to place the TLD circular chips. The circular surface of the TLDs is parallel to the seed long axis and is perpendicular to the slab plane [33, 34].

The measurements are carried out at distances of r = 0.5, 1, 1.5, 2, 3, 4, and 5 cm relative to the seed center. To minimize the interference of any of TLDs with regard

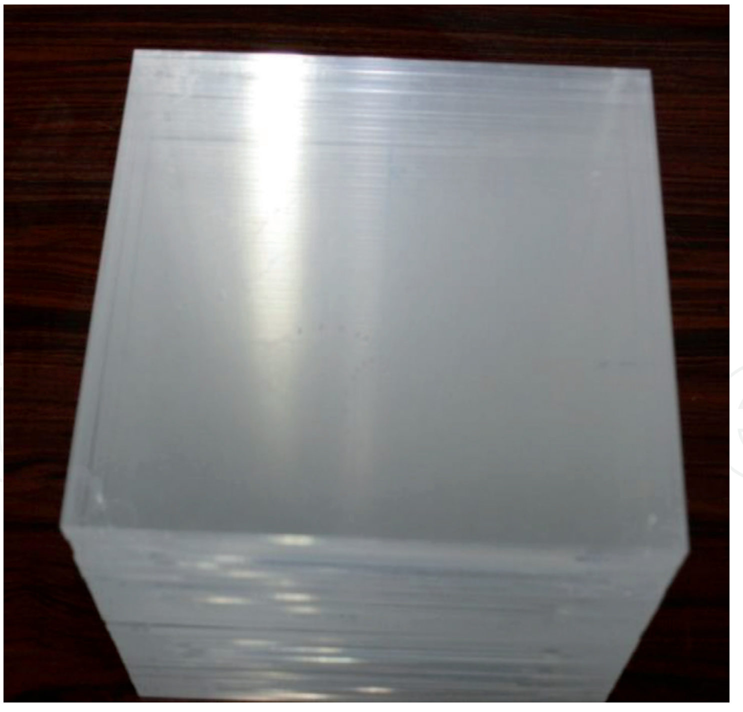

Figure 6.
Perspex phantom slabs.

Figure 7.
Central slabs of Perspex phantoms used for the experimental determination of radial dose function values.

to the response by other TLD chips, the measurement is performed in a spiral configuration [6, 8, 35, 36].

In this study, 28 TLDs (4 at each radial distance) were used for every single experiment to prevent the shadowing effect due to the configuration and the design of the phantom. To improve the statistical quality of the data, the experiment was repeated several times.

The other phantom is shown in **Figure 8**. This phantom has been used for the measurement of the anisotropy function of the brachytherapy seed. It has the same dimensions as the first phantom but differs in the configuration of the source in that. The source is placed parallel to the central slab plane with its long axis.

The TLDs are placed at radial distances of r = 1.5, 2, 3, and 5 cm relative to the seed center and also lie at the polar angles θ ranging from 0 to 330° in 30° increments with respect to the seed long axis. The measurements were performed with 48 holes containing TLDs since it was found that for the experimental anisotropy function

Figure 8.
Central slabs of Perspex phantoms used for the experimental determination of anisotropy function values.

determination at a specific point, shadowing effects due to the TLDs that lie at the same polar angle do not affect results. This is due to the definition of anisotropy function that normalizes dose rate at a particular (r, θ) point to the dose rate at the corresponding point along the transverse source bisector, (r, 90°). Therefore, since shadowing was found similar at any polar angle for the same radial distance, the overall effect is canceled out in the calculation of an anisotropy function [12].

4. Conclusion

This chapter presents the application of the cyclotron in brachytherapy by the production of radioisotopes such as Palladium-103.

In this chapter, production of the ^{103}Pd via cyclotron has been presented. **103Pd** is used in permanent low-dose radiation brachytherapy. So preparation of the brachytherapy source having ^{103}Pd radioisotope has also been discussed.

^{103}Pd production is performed via the ^{103}Rh(p,n)^{103}Pd reaction by 18 MeV protons for 15 h at 200 μA beam current. The optimum energy range and the thickness of the rhodium target are calculated by the several computer codes (ALIS/ASH, TALYS, EMPIRE). Several codes have been used to increase the accuracy of the calculations. To use the ^{103}Pd as brachytherapy source, the resin beads which are loaded by ^{103}Pd are encapsulated inside the titanium capsule, and then the capsules are implanted into the cancerous area. So, after the chemical separation process, ^{103}Pd radioisotope is absorbed uniformly in the resin Amberlite®IR-93, (20–50 mesh) bead to encapsulate them inside the titanium casing.

According to the American Association of Physicists in Medicine (AAPM) Radiation Therapy Committee recommendation, the dosimetric parameters of all new interstitial brachytherapy sources with energies less than 50 keV should be determined by two independent verifications, experimental measurements and theoretical calculations. The method for the theoretical calculation of the brachytherapy seed has been previously explained in Refs.s [6, 9]. In this study, the experimental measurement method, the design, and dimension of the phantom and configuration of the TLDs have also been explained.

Author details

Pooneh Saidi[1]* and Mahdi Sadeghi[2]

1 Parsikan Iran Engineering and Management Consultants, Tehran, Iran

2 Medical Physics Department, School of Medicine, Iran University of Medical Sciences, Tehran, Iran

*Address all correspondence to: poonehsaidi@gmail.com

References

[1] Khan F. Handbook of the Physics of Radiation Therapy. Baltimore: Williams and Wilkins; 2009. pp. 36-53

[2] Schlyer DJ, Van den Winkel P, Ruth TJ, Vora MM. Cyclotron produced radionuclides: Principles and practice. In: Technical Reports Series No. 465. Vienna: IAEA; 2008. pp. 31-57

[3] Simone Manenti S, del Carmen M, Santoro A, Cotogno G, Duchemin C, Haddad F, et al. Excitation function and yield for the 103Rh(d,2n)103Pd nuclear reaction: Optimization of the production of palladium-103. Nuclear Medicine and Biology. 2017;**49**:30-37

[4] Baltas D, Sakelliou L, Zamboglou N. The Physics of Modern Brachytherapy for Oncology. New York: Taylor & Francis Group; 2007. p. 165

[5] Sadeghi M, Enferadi M, Shirazi A. External and internal radiation therapy: Past and future directions. Journal of Cancer Research and Therapeutics. 2010;**6**:239-248

[6] Saidi P, Sadeghi M, Tenreiro C. Theory and applications of Monte Carlo simulations. In: Chan VWK, editor. Variance Reduction of Monte Carlo Simulation in Nuclear Engineering Field, Ch. 7. London: Intech; 2013. pp. 153-172. DOI: 10.5772/53384

[7] Saidi P, Sadeghi M, Shirazi A, Tenreiro C. Monte Carlo calculation of dosimetry parameters for the IR08-103Pd brachytherapy source. Medical Physics. 2010;**37**:2509-2515. DOI: 10.1118/1.3416922

[8] Saidi P, Sadeghi M, Tenreiro C. Experimental measurements and Monte Carlo calculations for 103Pd dosimetry of the 12 mm COMS eye plaque. Physica Medica. 2013;**29**:286-294. DOI: 10.1016/j.ejmp.2012.04.002

[9] Sadeghi M, Saidi P, Tenreiro C. Dosimetric characteristics of the brachytherapy sources based on Monte Carlo method. In: Mode CJ, editor. Applications of Monte Carlo Methods in Biology, Medicine and Other Fields of Science, Ch. 10. London: Intech; 2011. pp. 155-176. DOI: 10.5772/15884

[10] Saidi P, Sadeghi M, Enferadi M, Aslani G. Investigation of palladium-103 production and IR07-103Pd brachy-therapy seed preparation. Annals of Nuclear Energy. 2011;**38**:2168-2173

[11] Sadeghi M, Shirazi B. Extraction separation of no carrier- added ^{103}Pd from irradiated Rh target, Cu and Zn using α-furyldioxime, dimethylglyoxime and α-benzildioxime. Applied Radiation and Isotopes. 2008;**66**:1810-1813

[12] Sadeghi M, Shirazi B, Shadanpour N. Solvent extraction of no-carrier-added 103-Pd from irradiated rhodium target with α-furyldioxime. Journal of Radioanalytical and Nuclear Chemistry. 2006;**269**:223-225

[13] Broeders CHM, Konobeyev A, Kocrovin YA, Blann VPM. Pre-compound and Evaporation Model Code System for Calculation of Excitation Functions, Energy and Angular Distributions of Emitted Particles in Nuclear Reactions at Intermediate Energies. Frschungszentrum Karlsruhe Report FZKA. Hannover; 2006. p. 7183

[14] Koning AJ, Hilaire S, Duijvestijn M. TALYS-1.2: A Nuclear Reaction Program, User Manual. Netherlands: NRG; 2009

[15] EXFOR/CSISRS. 2011. Experimental Nuclear Reaction Data. Available from: http://wwwnds.iaea.org/exfor

[16] Koning AJ, Rochman D. TENDL-2010: TALYS-Based Evaluated Nuclear

Data Library. The Netherlands: Nuclear Research and Consultancy Group (NRG) Petten; 2010. Available from: http://www.talys.eu/tendl-2010

[17] Saidi Bidokhti P, Sadeghi M, Fateh B, Matloobi M, Aslani G. Nuclear data measurement of 186-Re production via various reactions. Nuclear Engineering and Technology. 2010;**42**(5):600-607

[18] Sadeghi M, Enferadi M. Nuclear model calculations on the production of 119Sb via various nuclear reactions. Annals of Nuclear Energy. 2011;**38**:825-834

[19] Büyükuslu H, Kaplan A, Tel E, Aydin A, Yildırım G, Bolukdemir MH. Theoretical cross-sections of ^{209}Bi, ^{232}Th, ^{235}U, and 238U on deuteron-induced reactions. Annals of Nuclear Energy. 2010;**37**:534-539

[20] Herman M, Capote R, Zerkin V, Trkov A, Wienke H, Sin M, et al. EMPIRE Modular System for Nuclear Reaction Calculations (version: 3.1 Rivoli). 2011. Available from: https://ndclx4.bnl.gov/gf/project/empire/

[21] Ziegler JF, Biersack JP, Littmark U. The Code of SRIM, the Stopping and Range of Ion in Matter. New York, USA: IBM-Research; 2006

[22] Saidi P, Sadeghi M. Theory, application and implementation of Monte Carlo method in science and technology. In: Bidokhti PS, editor. Modeling, Simulation, and Dosimetry of 103-Pd Eye Plaque Brachytherapy, Ch. 2. London: Intech; 2019. pp. 19-38. DOI: 10.5772/intechopen.78141

[23] Raisali G, Ghonchehnazi MG, Shokrani P, Sadeghi M. Determination of the geometry function for a brachytherapy seed, comparing MCNP results with TG-43U1 analytical approximations. Nukleonika. 2008;**53**:45-49

[24] Ataeinia V, Raisali G, Sadeghi M. Determination of dosimetry parameters of ADVANTAGETM 103Pd brachytherapy seed using MCNP4C computer code. Nukleonika. 2009;**54**:181-187

[25] Saidi P, Sadeghi M, Hosseini SH. Thermoluminescent dosimetry of the IR06-103Pd brachytherapy source. Journal of Applied Clinical Medical Physics. 2011;**12**(4):286-295. DOI: 10.1120/jacmp.v12i4.3581

[26] Harper PV, Lathrop K, Need JL. The thick target yield and excitation function for the reaction 103Rh(p,n)103Pd. Nuclear Science. 1961;**15**:124

[27] Hansen LF, Albert RD. Statistical theory predictions for 5 to 11 MeV (p,n) and (p,p') nuclear reactions in 51V, 59Co, 63Cu, 65Cu, and 103Rh. Physics Review. 1962;**128**:291-299

[28] Hermanne A, Sonck M, Fenyvesi A, Daraban L. Study of production of ^{103}Pd and characterisation of possible contaminants in the proton irradiation of 103Rh up to 28 MeV. Nuclear Instruments & Methods. 2000;**B170**:281-292

[29] Sudar S, Cserpak F, Qaim SM. Measurements and nuclear model calculations on proton-induced reactions on Rh-103 up to 40-MeV-evaluation of the excitation function of the Rh-103(p,n)Pd-103 reaction relevant to the production of the therapeutic radionuclide Pd-103. Applied Radiation and Isotopes. 2002;**56**:821-831

[30] Tárkányi F, Hermanne A, Király B, Takacs S, Ditrói F, Csikai J, et al. New cross-sections for production of 103Pd; review of charged particle production routes. Applied Radiation and Isotopes. 2009;**67**:1574-1581

[31] Hermanne A, Sonck M, Takacs S, Tárkányi F, Shubin FY. Study on alternative production of 103Pd and characterisation of contaminant sin the deuteron irradiation of 103Rh up to 21 MeV. Nuclear Instruments & Methods. 2002;**B187**:3-14

[32] Duggan L, Hood C, Warren-Forward H, Haque M, Kron T. Variation in dose response with X-ray energy of LiF:Mg, Cu, P thermoluminescence dosimeters: Implications for clinical dosimetry. Physics in Medicine and Biology. 2004;**49**(18):3831-3845

[33] Meigooni AS, Gearheart DM, Sowards K. Experimental determination of dosimetric characteristics of bests 125I brachytherapy source. Medical Physics. 2000;**27**(9):2168-2173

[34] Meigooni AS, Sowards K, Soldano M. Dosimetric characteristics of the intersource 103-palladium brachytherapy source. Medical Physics. 2000;**27**(5):1093-1099

[35] Hosseini SH, Sadeghi M, Ataeinia V. Dosimetric comparison of four new designs 103-Pd brachytherapy sources: Optimal design using silver and copper rod cores. Medical Physics. 2009;**36**(7):3080-3085

[36] Sadeghi M, Hosseini SH, Raisali G. Experimental measurements and Monte Carlo calculations of dosimetric parameters of the IRA1-103Pd brachytherapy source. Applied Radiation and Isotopes. 2008;**66**(10):1431-1437